European Journal of Pharmaceutics and Biopharmaceutics 137 (2019) 23–36

Contents lists available at ScienceDirect

European Journal of Pharmaceutics and Biopharmaceutics

journal homepage: www.elsevier.com/locate/ejpb

Research paper

Human primary macrophages scavenge AuNPs and eliminate it through exosomes. A natural shuttling for nanomaterials

Mariantonia Logozzi[a,1], Davide Mizzoni[a,1], Beatrice Bocca[b], Rossella Di Raimo[a], Francesco Petrucci[b], Stefano Caimi[b], Alessandro Alimonti[b], Mario Falchi[c], Francesco Cappello[d,e], Claudia Campanella[d,e], Celeste Caruso Bavisotto[d,e,f], Sabrina David[d,e], Fabio Bucchieri[d,e], Daniela F. Angelini[g], Luca Battistini[g], Stefano Fais[a,*]

[a] Department of Oncology and Molecular Medicine, Istituto Superiore di Sanità, Viale Regina Elena 299, 00161 Rome, Italy
[b] Department of Environment and Health, Istituto Superiore di Sanità, Viale Regina Elena 299, 00161 Rome, Italy
[c] National AIDS Center, Istituto Superiore di Sanità, Viale Regina Elena 299, 00161 Rome, Italy
[d] Department of Experimental Biomedicine and Clinical Neuroscience, Section of Human Anatomy, University of Palermo, 90127 Palermo, Italy
[e] Euro-Mediterranean Institute of Science and Technology (IEMEST), 90136 Palermo, Italy
[f] Institute of Biophysics, National Research Council, 90143 Palermo, Italy
[g] Neuroimmunology Unit, IRCCS Santa Lucia Foundation, 00179 Rome, Italy

ARTICLE INFO

Keywords:
Nanotechnology
Nanoparticles
Exosome
SP-ICP-MS
NTA

ABSTRACT

The use of nanomaterials is increasing but the real risk associated with their use in humans has to be defined. In fact, nanomaterials tend to accumulate in organs over a long period of time and are slowly degraded or eliminated by the body. Exosomes are nanovesicles actively shuttle molecules, including chemical products and metals, through the body. Macrophages scavenge the body from both organic and inorganic substances, and they use to release high amounts of exosomes. We hypothesized that macrophages may have a role in eliminating nanomaterials through their exosomes. We treated human primary macrophages with 20 nm gold nanoparticles (AuNPs), analyzing the presence of AuNPs in both cells and the released exosomes by the implementation of different techniques, including SP-ICP-MS and NTA. We showed that macrophages endocytosed AuNPs and released them through exosomes. Our study on one hand provide the evidence for a new methodology in the early identification of the nanomaterials levels in exposed subjects. On the other hand we depict a way our body shuttle virtually intact nanoparticles through macrophage-released exosomes.

1. Background

Nanotechnology is rapidly expanding and there are many products containing nanomaterials, such as batteries, coatings, antibacterial clothes, cosmetics and food products [1].

Despite the increasing use of nanomaterials in medicine, cosmetics, agro-food, renewable energy and biomedical devices [2,3], there are still no clear and definitive rules that regulate their use and define the real risks for the organism and the environment [4–6].

In 2011, the "Recommendation on the definition of a nanomaterial (2011/696/EU)" adopted a definition of a nanomaterial as "a natural, incidental or manufactured material containing particles, in an unbound state or as an aggregate or as an agglomerate and where, for 50% or more of the particles in the number size distribution, one or more external dimensions is in the size range 1–100 nm" [7]. Nanomaterials are present in nature, for example in the emissions of volcanoes, or they can be by-products of human activities, such as diesel engine exhaust fumes or tobacco smoke.

The SCENIHR scientific committee [8] noted that there are proven health risks associated with some manufactured nanomaterials because through inhalation, ingestion, injection or cutaneous exposure they can enter the bloodstream and consequently the various organs: lungs, liver, spleen, lymph nodes, bone marrow, kidneys, heart, brain and skeleton, in particular accumulating in the *reticuloendothelial system* (RES) [2,4,9,10]. RES is part of the immune system and is characterized by three types of cells: reticular, macrophages and Kupffer cells.

So far, most *in vivo* studies indicate that nanomaterials have a high tendency to accumulate in organs over a long period of time and are

* Corresponding author.
E-mail address: stefano.fais@iss.it (S. Fais).
[1] These authors contribute equally to this work.

https://doi.org/10.1016/j.ejpb.2019.02.014
Received 31 October 2018; Received in revised form 11 February 2019; Accepted 15 February 2019
Available online 16 February 2019
0939-6411/

slowly degraded or eliminated by the body [10,11]. In particular, nanomaterials < 5 nm can be removed from the blood by renal clearance, those of 10–20 nm through rapid hepatic diffusion [10,12], nanomaterials between 20 and 200 nm can remain in circulation for a prolonged period of time, while nanomaterials > 200 nm are filtered in the sinusoids of the spleen [10,13] are recognized and eliminated by tissue macrophages [10,14]. Therefore, the accumulation of nanomaterials in tissues and organs makes their further biodegradation or excretion difficult, inducing high toxicity [10,11] above all through excessive production of ROS (reactive oxygen species) [15–20]. The consequences can be cell damage through lipid peroxidation, protein alteration, DNA chain termination, interference with signaling functions and modulation of gene transcription, thus leading to inflammation, tissue damage, fibrosis, tumorigenesis, cardiovascular damage, kidney disease, neurodegeneration, lung disease, vasculopathy [16,21–28].

As a result of inhalation, toxic substances have been shown to come into contact with different types of lung cells, including epithelial cells, endothelial cells, alveolar macrophages, monocytes and circulating blood cells, leading to increased release and altered composition of extracellular vesicles (EVs), a class of vesicles to which exosomes belong, and they may contribute to the pathogenesis of chronic diseases, promoting inflammation [29,30], hypercoagulability [31,32], endothelial dysfunction [33,34], tissue remodeling [35,36] and angiogenesis [37,38].

The growing interest in exosomes in the field of nanomedicine is due both to their nano size (30–180 nm) and to their ability to transport molecules, such as proteins, lipids, viruses, prions, metabolites, nucleic acids, both constituents and cell-specific, able to induce a specific function in the target cells, both by a receptor-ligand bond and by membrane-membrane fusion and transfer of the content into the target cell [39–45].

Furthermore, exosomes have the capacity to carry drugs such as cisplatin and acridine orange [46,47] and play a key role in the metastatic process of tumors [48], thus representing in this case a paracrine diffusion system of malignancy.

Exosomes act as Trojan horses for the dissemination and intercellular communication of natural nanoparticles (such as viruses) [49–51]. In fact, following exposure to magnetic iron oxide nanoparticles (MIONs), a significant number of exosomes can be generated in a dose-dependent manner in the alveolar region of BALB/c mice. These exosomes are rapidly eliminated from the alveoli in the systemic circulation and largely transfer their signals to the immune system, inducing dendritic cell maturation and activation of the splenic T cells [52].

The 1908 Nobel Prize (together with Paul Ehrlich) and mentor of modern immunology Metchnikoff, in his initial studies on phagocytosis, started from investigations of unicellular organisms, which actually ingest other microorganisms in order to feed upon the “ingested material”. Only later he discovered the existence of circulating cells that used phagocytosis to protect the higher organisms from external agents, a milestone discovery of modern immunology. However, the Metchnikoff’s discovery changed the paradigm “Eat to feed” in “Eat to defend”, reviewed in [53]. Today we know much more on professional phagocytes, such as macrophages. We know for instance that peripheral blood monocytes are very plastic cells with a high potential of differentiating in either macrophages, dendritic cells, endothelial-like cells, muscle-like cells or multinucleated giant cells [54,55]. However, we know also that when peripheral blood monocytes get to a tissue and become macrophages they do not have potential to differentiate in another cell anymore [56,57]. Thus, human macrophages are naturally involved in the mechanisms of “purification” of our organism from both organic and inorganic substances and able to secrete a large number of exosomes. On this basis we hypothesized that such cells are able to eliminate nanomaterials through the exosomes they release, transporting them to different organs or tissues.

For the above reasons in this paper we wanted to investigate the involvement of primary monocytes-derived human macrophages in the elimination of nanomaterials through exosomes release. To this purpose we exploited a detection system of the metal nanoparticles potentially contained in the macrophage-released exosomes through the integration and implementation of different techniques such as SP-ICP-MS (Single Particle-Inductively Coupled Plasma-Mass Spectrometry) and NTA (Nanoparticle Tracking Analysis).

As a model of nanoparticles we used 20 nm gold nanoparticles (AuNPs) because it has been shown that nanomaterials with sizes ranging from 20 to 200 nm can remain in circulation for a prolonged period of time and then be phagocytosed and eliminated by macrophages [10]. Moreover, AuNPs are extensively used in diagnosis and therapy of many diseases. In fact, AuNPs have aroused considerable interest in medical applications, and they are widely used in imaging techniques, drug delivery, medical devices and as photothermal agents or tumor markers [58]. The AuNPs chosen for the treatment of primary human macrophages have a diameter of 20 nm, consistent with the exosomes size, and physical and optical properties that make them analyzable using various methods. Actually, it was necessary to combine complementary techniques to obtain a detailed view including both qualitative and quantitative assessments. Therefore we developed and applied different detection methods such as Transmission Electron Microscopy (TEM), Laser scanning confocal microscopy (LSCM), NTA and SP-ICP-MS to obtain a complete view of AuNPs intracellular uptake and exosome elimination.

SP-IC-MS identified AuNPs in lysed cells and exosomes, while the (NTA) demonstrated the presence of AuNPs in intact exosomes, suggesting the possibility of simultaneously using the two analytical techniques to monitor the levels of nanomaterials in exosomes of exposed subjects.

2. Materials and methods

2.1. Isolation and differentiation of primary human monocytes/macrophages from peripheral blood

Buffy coats of 5 healthy donors were provided by Centro Trasfusionale Universitario Azienda Policlinico Umberto I in Rome, Italy (the study was approved by the ethical committee of Istituto Superiore di Sanità, Rome, Italy, and donors gave written-informed consent to participate). Primary human monocytes were obtained after the separation of PBMCs (Peripheral Blood Mononuclear Cell) through a gradient Lympholyte®-H from the *buffy coat* of healthy donors. PBMCs were cultured in RPMI 1640 medium with 20% FBS (*Fetal Bovine Serum*) and antibiotics, at 37° C with 5% CO_2. The macrophages were selected by adhesion to the plate. After the addition of fresh culture medium the monocytes were allowed to differentiate into macrophages for 7–10 days.

2.2. Gold nanoparticles (AuNPs)

The AuNPs (SIGMA – ALDRICH) have a certified diameter of 20 nm, O.D. 1 and are stabilized in citrate buffer. The AuNPs have an absorption maximum at a 518–522 nm wavelength (λmax) and greater stability that make them ideal in physical and optical applications.

Human macrophages were treated by resuspending AuNPs at different concentrations in RPMI 1640 culture medium with 10% exo-free FBS. Using the SP-ICP-MS we evaluated the stability of the AuNPs standard with a diameter of 20 nm.

2.3. Single Particle-Inductively Coupled Plasma-Mass Spectrometry (SP-ICP-MS)

The AuNPs standard at 20 nm diameter (Sigma Aldrich, Darmstadt, Germany), stabilized in citrate buffer, was used for method optimization and sample analysis. The standard was diluted in deionized

Table 1
Operating conditions for AuNPs analysis by SP-ICP-MS.

SP-ICP-MS instrument	iCAP-Q ICP-MS (thermo fisher)
Plasma power	1500 W
Nebulizer and flow	PFA-ST; 0.35 mL/min
Nebulization efficiency	4%
Sensitivity (cps/μg/L)	137,000
Mass monitored	^{197}Au
Dwell time	5 msec
Acquisition mode; time	Standard; 60 sec
Density	19.3 g/cm^3

ultrapure water and sonicated in ultrasonic bath for 20 min before the analysis to prevent subsequent agglomeration. NPs analysis was performed using an ICP-MS (iCAP™Q, Thermo Scientic, Bremen, Germany) operated in Single Particle (SP) mode. The Thermo Scientific™ Qtegra software was used to automatically generate particle diameter information (in nm), particle number concentration (in particles / mL), and size detection limit (LoD in nm). The principle of SP-ICP-MS measurements is that the height (in counts per second, cps) of spikes, called Single-Particle Events (SPEs), is proportional to particle size and the number of spikes per run is proportional to the number of particles in the sample. While, the background signal (BG) represented the dissolved Au ions. The operating conditions and method parameters are listed in Table 1. The dwell time was set at 5 msec, the ^{197}Au isotope was measured and the run time was 60 s per sample. To calculate the sensitivity of the ICP-MS system, a calibration stock solution of Au dissolved in ionic form was used (CPAChem, C.P.A. Ltd., Stara Zagora, Bulgaria). The transport efficiency of the ICP-MS sample introduction system was calculated by analyzing the 20 nm AuNP standard, using the dimension-based efficiency approach [59]. In the SP-ICP-MS analysis, Au mass (m) was measured first and then converted into Au diameter (D) knowing Au density (19.3 g/cm^3) and assuming as spherical the Au particle, according to the SP-ICP-MS theory [59]. To study the recovery method, the 20 nm Au standard was added at a concentration of 250,000 particles/mL in both water and RPMI + 10% serum. To evaluate the stability of AuNPs, in water and in culture medium, the added (spiked) samples were analyzed at T0 and after 24 h (T24) and evaluated by detecting the change in particle size. Cell and exosome lysates treated at different doses of AuNPs (0, 0.1, 1.0, 10 and 50 μM) were diluted 1:1000 in ultrapure deionized water, sonicated in an ultrasonic bath for 20 min and analyzed using the same SP-ICP-MS method, described in Table 1.

2.4. Laser scanning confocal microscopy (LSCM)

The isolated PBMCs were plated on microscopy slides and then after 7–10 days, following their differentiation into macrophages, were treated for 24 h with a concentration of 10 μM AuNPs. Subsequently, the cells were fixed in 3% paraformaldehyde for 10 min at room temperature, washed with PBS and transferred onto object slides with ProLong + DAPI. The images were acquired with an FV1000 confocal microscope (Olympus, Tokyo, Japan), using a planapo lens (Olympus) 60x oil A.N. 1.42. AuNPs emissions were recorded between 480 and

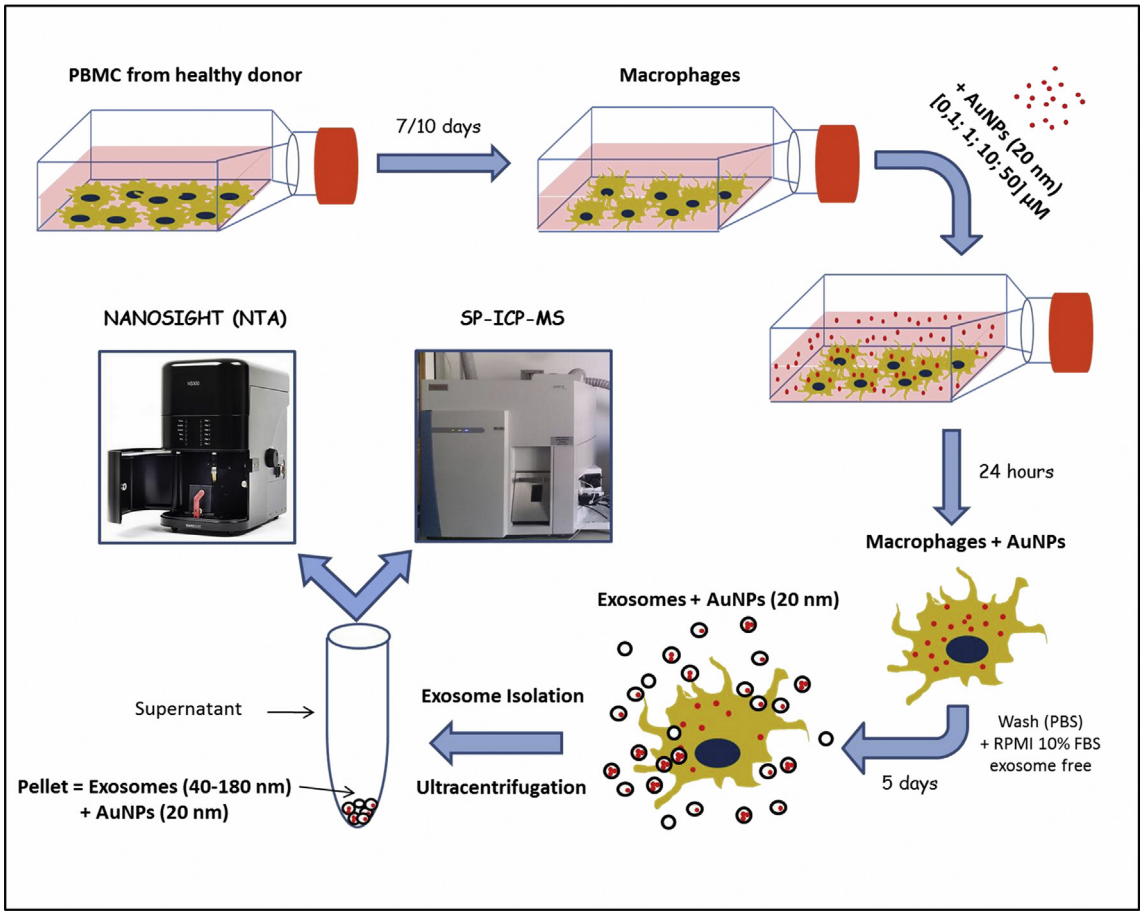

Fig. 1. Experimental scheme of treatment of primary human macrophages with AuNPs. Primary human macrophages differentiate from Monocytes isolated from PBMCs (Peripheral Blood Mononuclear Cell) from human healthy donors were treated for 24 h with different concentrations of AuNP of 20 nm (0,1, 1, 10, 50 μM) and analyzed in confocal microscopy and transmission electron microscopy (TEM). After 5 days incubation with culture medium, the exosomes from human macrophages were isolated and analyzed by Single Particle Inductively Coupled Plasma Mass Spectrometry (SP-ICP-MS) and by Nanoparticle Tracking Analysis (NTA).

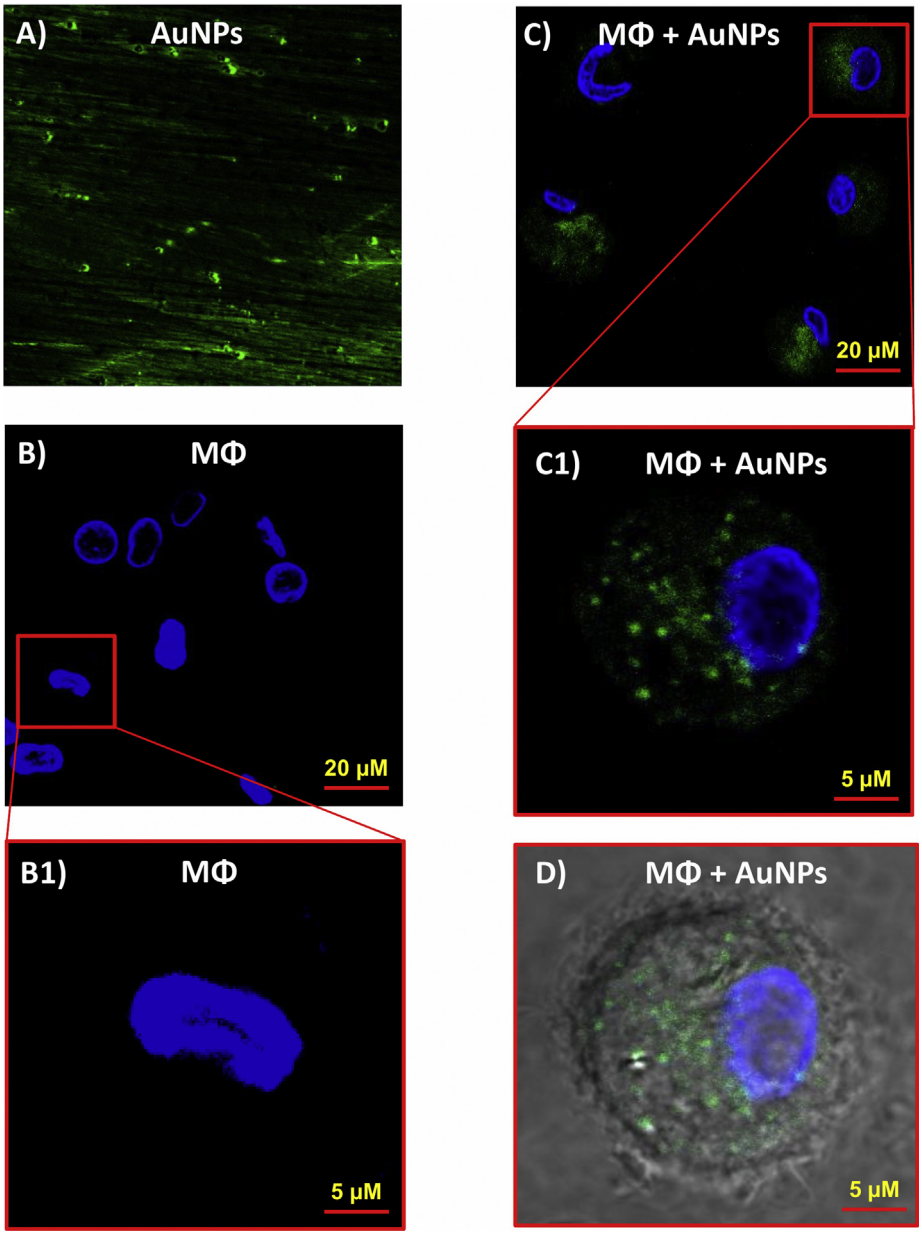

Fig. 2. Confocal microscopy to analyze the presence of AuNPs in primary human macrophages (MΦ). Primary human macrophages (MΦ) were labeled with AuNPs (20 nm) for 24 h with a concentration of 10 μM at 37 °C, then fixed in 3% paraformaledehyde, labeled with DAPI and observed in confocal microscope. (A) Fluorescence emission of AuNPs at wavelengths of 480–520 nm. (B and B1) Primary human macrophages not treated with AuNPs (control). (C, C1 and D) Primary human macrophages treated with AuNPs.

520 nm with an Argon Ion Laser (488 nm). DAPI emissions were recorded between 415 and 485 nm with a DAPI Laser (408 nm). The images acquired have an optical thickness of 0.4 mm.

2.5. Transmission electron microscopy (TEM)

The differentiated primary human macrophages were treated for 24 h with a concentration of 10 μM of AuNPs.

The macrophage cultures (treated and untreated) were fixed in a 2.5% glutaraldehyde solution in phosphate buffer, pH 7.4, for 20 min at room temperature. Glutaraldehyde was removed and the cells were stored in phosphate buffer at 4 °C until the next steps. The cells were then fixed in 1% OsO4 for 2 h, dehydrated in a increasing series of ethanol, treated with propylene oxide for 30′, infiltrated with epoxy resin (Epon812, Electron Microscopy Science, Hatfield, PA, USA) in propylene oxide (1:3, 1:2 and 1:1 for 30 min at room temperature, respectively) and then inserted into Epon812 with DMP30. The resin was then polymerized in an oven at 60° C for 48 h. The ultra sections were cut with an ultramicrotome (Ultracut E, Reichert-Jung, Depew, NY, USA) and mounted on copper and gold grids and were contrasted with 7% of uranyl acetate in methanol and with Reynold's lead citrate before acquiring the transmission electron microscope images (JEM-1220; JEOL, Japan) as described below [60,61].

2.6. Isolation of exosomes

The supernatants of primary human macrophages were collected after 5 days of culture to isolate exosomes. The supernatants were subjected to serial centrifugations of 300*g* for 5 min, 1200*g* for 15 min, 12,000*g* for 30 min, and then ultracentrifuged at 110,000*g* for one hour in the Sorvall WX Ultracentrifuge Series (Thermo Fisher Scientific) to obtain the exosomal pellet, which was then washed in PBS and

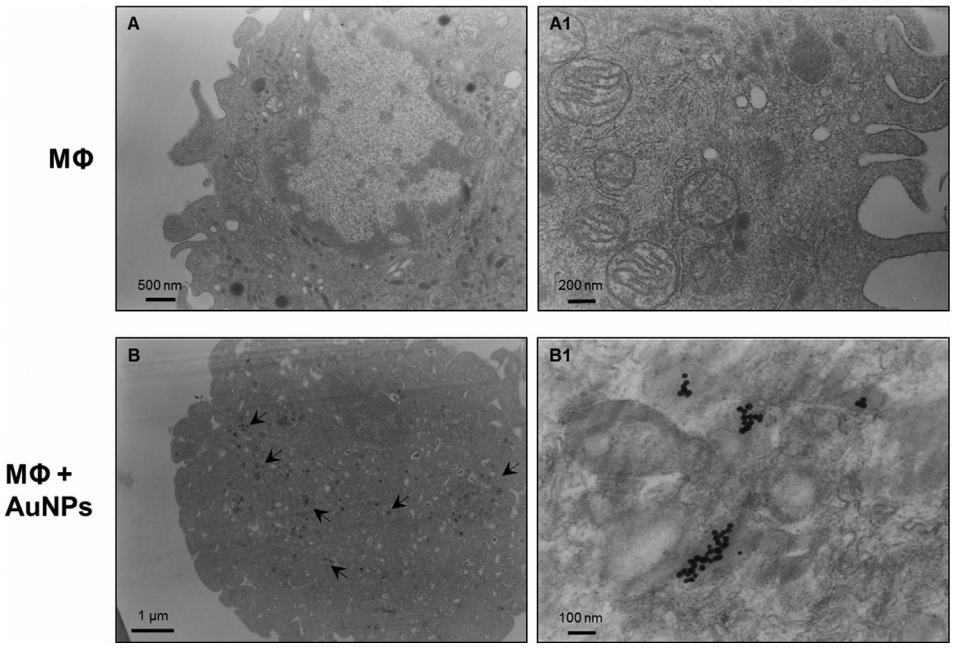

Fig. 3. Transmission electron microscopy (TEM) analysis to verify the internalization of AuNPs in treated macrophages. Electron microscopy analysis of macrophages showing the distribution of AuNPs. (A and A1) Representative image of macrophages untreated. (B) an electron photomicrographs demonstrated the positivity to AuNPs (indicated by black dots) on the inner membrane of an early endosome-like structure or possible MVBs (arrows). (B1) Higher magnifications demonstrated details.

resuspended in the appropriate buffer for subsequent analyzes [62].

2.7. Western blot analysis

Human macrophages untreated and treated for 24 h with 10 µM of AuNPs (20 nm) were lysed in CHAPS buffer 1x (Tris 10 mM pH 7.4, MgCl2 1 mM, ethyleneglycoltetraacetic acid (EGTA) 1 mM, CHAPS 0.5%, glycerol 10%, and phenylmethylsulfonylfluoride (PMSF) 1 mM) with protease (1 µg/mL leupeptin, 1 µg/mL pepstatin A, 1 µg/mL aprotinin, and PMSF 1 mM) incubated for 30 min on ice and centrifuged for 30 min at 12,000 rpm at 4 °C, thus removing cell debris and collecting the supernatant. Exosomes were lysed in CHAPS buffer 1x and processed as previously described. Protein concentration was determined using the Bradford protein assay (Bio-Rad Laboratories, Inc, Hercules, CA, USA). Thirty micrograms per sample were resolved on 10% acrylamide gel and transferred to a Protran BA85 nitrocellulose membrane (Schleicher & Schuell, Keene, NH, USA). Membranes were blocked overnight with 5% dry milk in PBS 1x. Blotting was performed employing anti-Tsg101 (4A10, GeneTex, Irvine, CA, USA) monoclonal antibody. After incubation with appropriate peroxidase-conjugated anti-immunoglobulin G (IgG; Amersham Biosciences, Milan, Italy), membranes were revealed by enhanced chemiluminescence (Pierce, Rockford, IL, USA).

2.8. Nanoscale flow cytometry

Exosomes purified from supernatants of human macrophages untreated and treated for 24 h with 10 µM of AuNPs (20 nm) were diluted in PBS in a final volume of 40 µl (1 mg/mL). Anti-human CD81 allophycocyanin (APC) conjugated (Beckman Coulter; Brea, CA, USA) and mouse anti-human CD9 phycoerythrin (PE) conjugated (M-L13, RUO (GMP) BD Biosciences, USA) were added to the exosome preparation at optimal pre-determined concentrations and left for 30 min at room temperature (RT). The samples were then acquired on the CytoFLEX flow cytometer (Beckman Coulter, Brea, CA, USA). The cytometer was calibrated using a mixture of non-fluorescent silica beads and fluorescent (green) latex beads with sizes ranging from 110 nm to 1300 nm. This calibration step enabled the determination of the sensitivity and resolution of the flow cytometer (fluorescent latex beads) and the size of extracellular vesicles (silica beads). All samples were acquired at low flow rate for the same amount of time in order to obtain an estimate of absolute counts of exosomes comparable between various samples. The analysis of the data was performed with the FlowJo software (FlowJo, LLC; Ashland, OR, USA) [47].

2.9. SP-ICP-MS analysis to evaluate the presence of AuNPs

Primary human macrophages differentiated after 7/10 days were treated for 24 h with concentrations of 0.1, 1, 10 and 50 µM of AuNPs. Following 5 washes with PBS, fresh culture medium was added and, after 5 days of incubation, exosomes from the supernatant were isolated and macrophages were collected. Cells and exosomes were resuspended in a lysis buffer, respectively AKT (NaCl 150 Mm, Tris 20 mM, NP40 1%, Glycerol 10%) and lysis buffer for exosomes (1% Triton X-100, 0.1% SDS, 0.1 M TRIS HCl) with protease inhibitors (Hoffman-La Roche).

Cellular and exosomal lysates were used for SP-ICP-MS analysis. This technique was used to detect and quantify AuNPs. When reaching the plasma, the particle generates a SPE that lasts about 300 µs: the introduction of a diluted suspension of NPs in the ICP-MS generates a pulse every time a single particle enters the plasma, is ionized and detected as an ion packet. Collecting the data resolved over time it is possible to examine both the numerical concentration and the dimensional distribution of the sample. The number of events (or spikes) per run is proportional to the number concentration of particles. The height (or intensity) of events is proportional to the size of the particles.

2.10. Nanoparticle Tracking Analysis (NTA)

Malvern NTA (NanoSight NS300) was used to measure the distribution and concentration of intact exosomes isolated from the cultures of primary human macrophages treated for 24 h with concentrations of 0.1, 1, 10 and 50 µM of AuNPs and not treated. The exosomes, isolated after 5 days of incubation with fresh culture medium, were resuspended in PBS and analyzed. Five 60-second videos were acquired and analyzed with the NTA 3.0 software (Malvern Instruments). The analysis is based on the Brownian motion of nanovescicles suspended in a liquid. The Brownian motion of each particle has been traced using the Stokes-Einstein equation:

$D^\circ = kT/6\pi\eta r$, where D° is the diffusion coefficient, $kT/6\pi\eta r = f_0$ is the particle friction coefficient, in the case of a spherical particle of radius r which moves with uniform velocity in a continuous viscosity

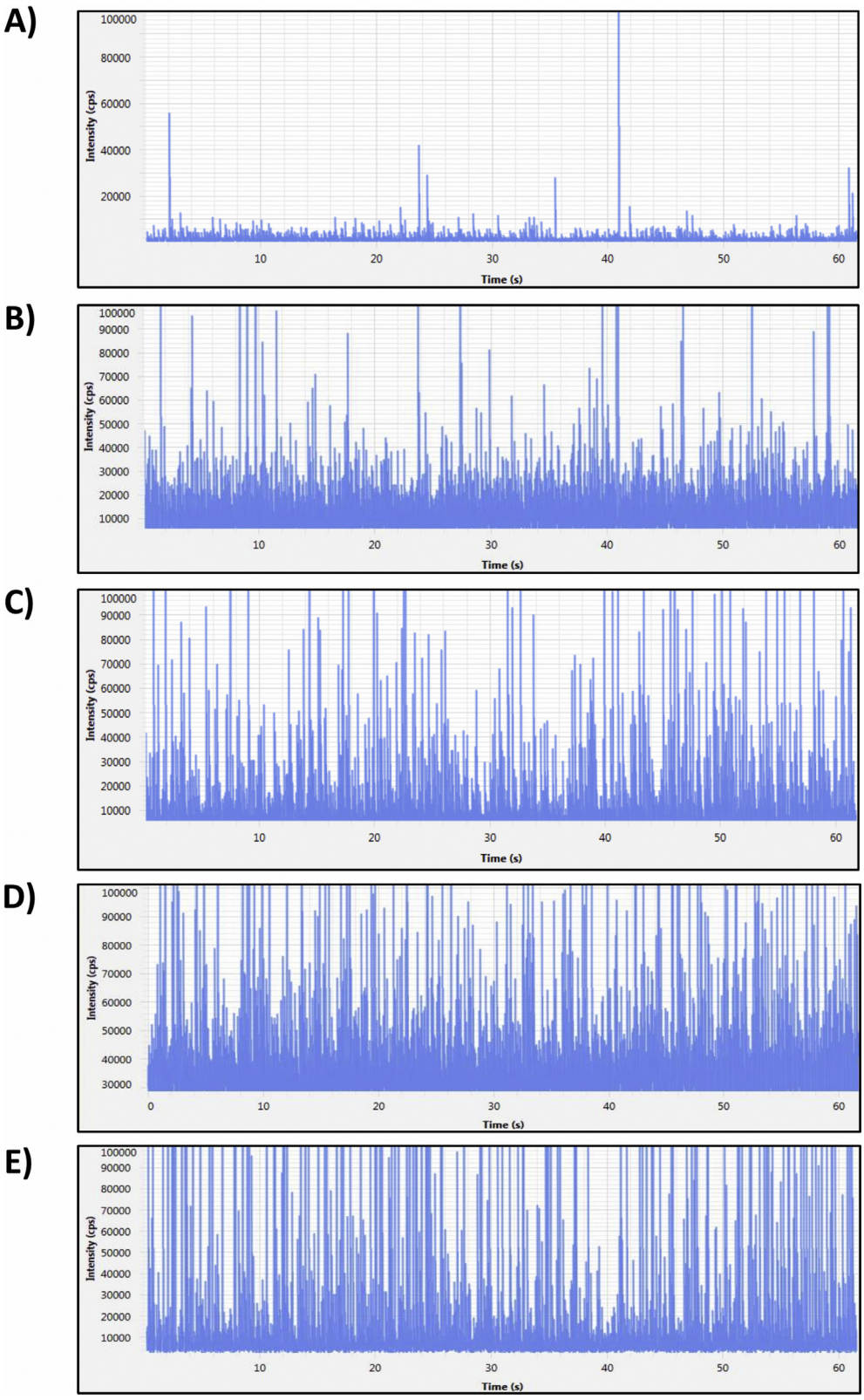

Fig. 4. Single Particle Events (SPEs) of AuNPs 20 nm in primary human macrophages lysates by SP-ICP-MS analysis. SPEs of 20 nm AuNPs in primary human macrophages treated at different doses; the number of SPEs is proportional to the number concentration of AuNPs, and the intensity (cps) of SPEs is proportional to the size of AuNPs. (A) 0 μM (control), (B) 0.1 μM, (C) 1.0 μM, (D) 10 μM and (E) 50 μM.

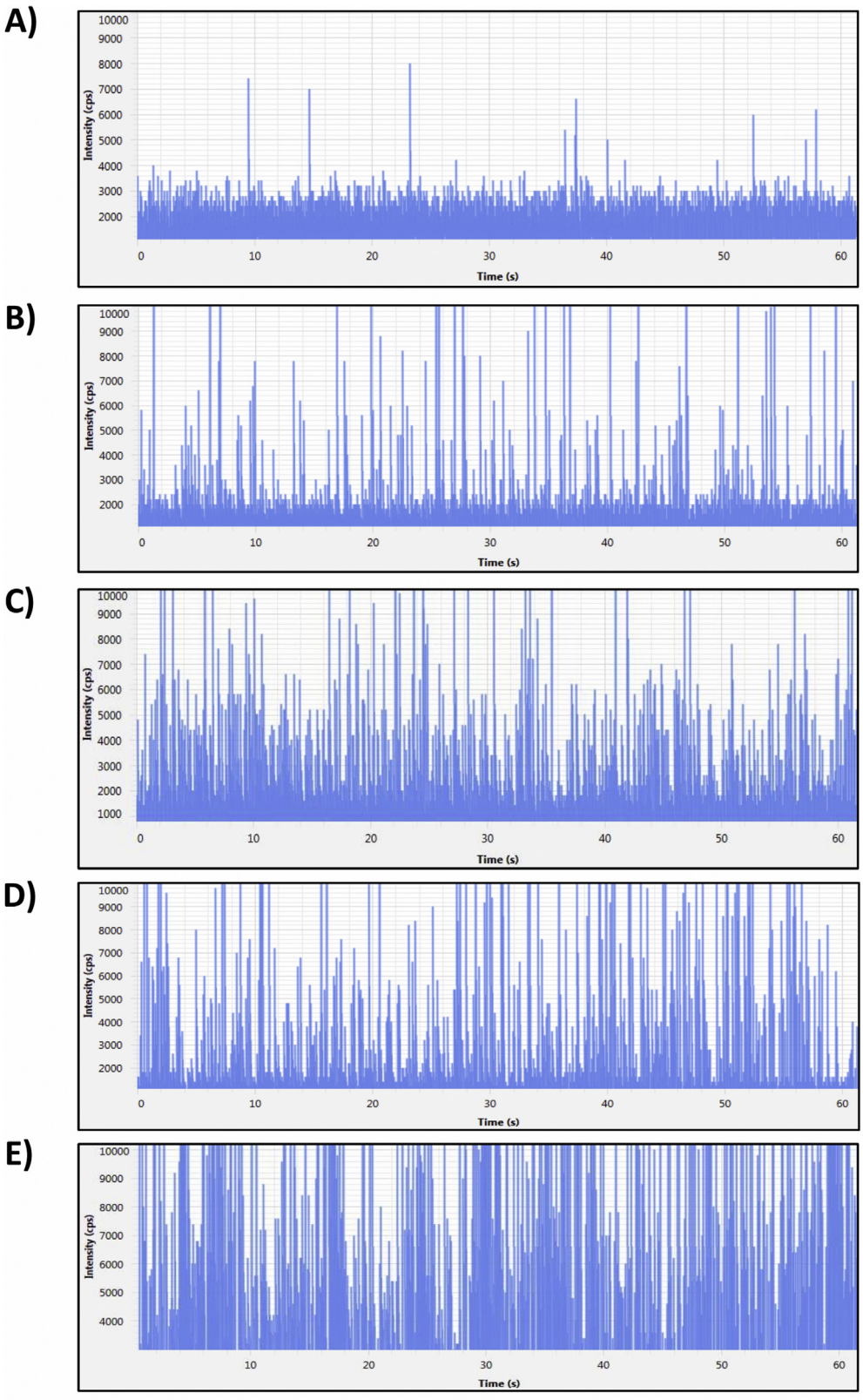

Fig. 5. Single Particle Events (SPEs) of AuNPs in exosomes lysates by SP-ICP-MS analysis. SPEs of 20 nm AuNPs in exosomes released by primary human macrophages treated at different doses; the number of SPEs is proportional to the number concentration of AuNPs, and the intensity (cps) of SPEs is proportional to the size of AuNPs. (A) 0 μM (control), (B) 0.1 μM, (C) 1.0 μM, (D) 10 μM and (E) 50 μM.

Table 2
AuNPs in lysates of macrophages and exosomes at the different doses by SP-ICP-MS.

Macrophages lysates		
Dose (μM)	Diameter (nm)	Concentration (particles/ml)
0.1	24.0	5.17E + 07
1	21.8	5.00E + 08
10	21.4	4.86E + 09
50	22.2	1.27E + 10
Exosomes lysates		
Dose (μM)	Diameter (nm)	Concentration (particles/ml)
0.1	22.0	2.15E + 07
1	20.5	2.79E + 08
10	21.0	2.37E + 09
50	20.6	4.02E + 09

fluid η, k is the Boltzmann constant, T is the absolute temperature [63].

3. Results

3.1. Treatment of primary human macrophages with AuNPs

Monocytes isolated from PBMCs (Peripheral Blood Mononuclear Cell) from human healthy donors were allowed to differentiate into macrophages for 7–10 days (Fig. 1). The differentiated primary human macrophages were treated for 24 h with a concentration of 10 μM AuNPs with a diameter of 20 nm for analysis by laser scanning confocal microscopy (LSCM) and transmission electron microscopy (TEM) in order to identify the possible presence and distribution of AuNPs within the treated macrophages. To analyze the possible release of AuNPs by the exosomes, two innovative and complementary techniques were used: Single Particle Inductively Coupled Plasma Mass Spectrometry (SP-ICP-MS) and Nanoparticle Tracking Analysis (NTA). Primary human macrophages were treated for 24 h with increasing concentrations of AuNPs (0.1, 1, 10, 50 μM) and, following 5 washings with PBS and 5 days of incubation with fresh culture medium at 10% Exosomes-free FBS, exosomes were isolated by serial centrifugation and ultracentrifugation for subsequent analysis by SP-ICP-MS and NTA.

Consistently and in accordance with previous studies [47] macrophages were treated with AuNPs for 24 h to obtain the lowest cell

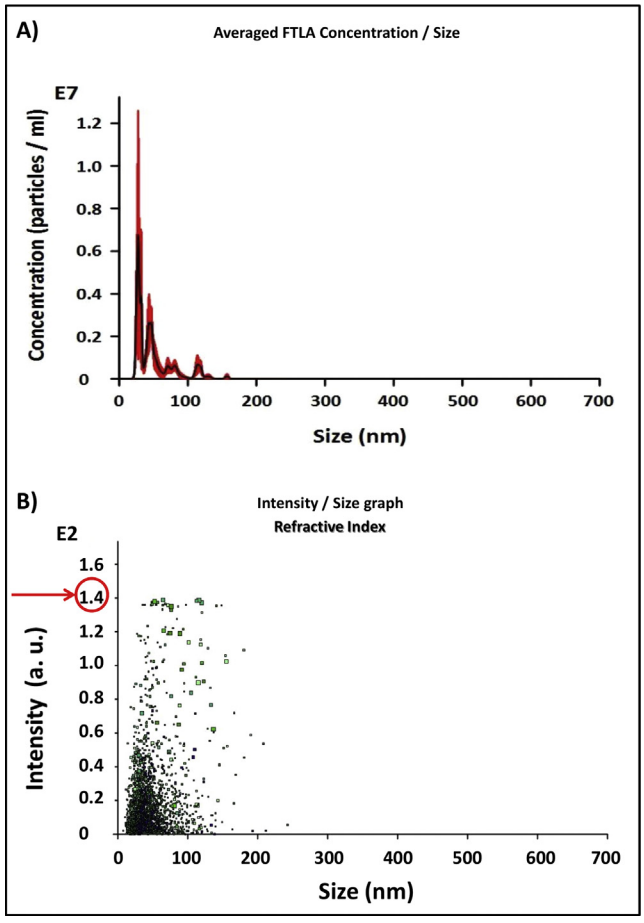

Fig. 7. Nanoparticle Tracking Analysis (NTA) of real 20 nm size of AuNPs. NTA for distribution, concentration (absolute count) and refractive index of real 20 nm size of AuNPs diluted in water.

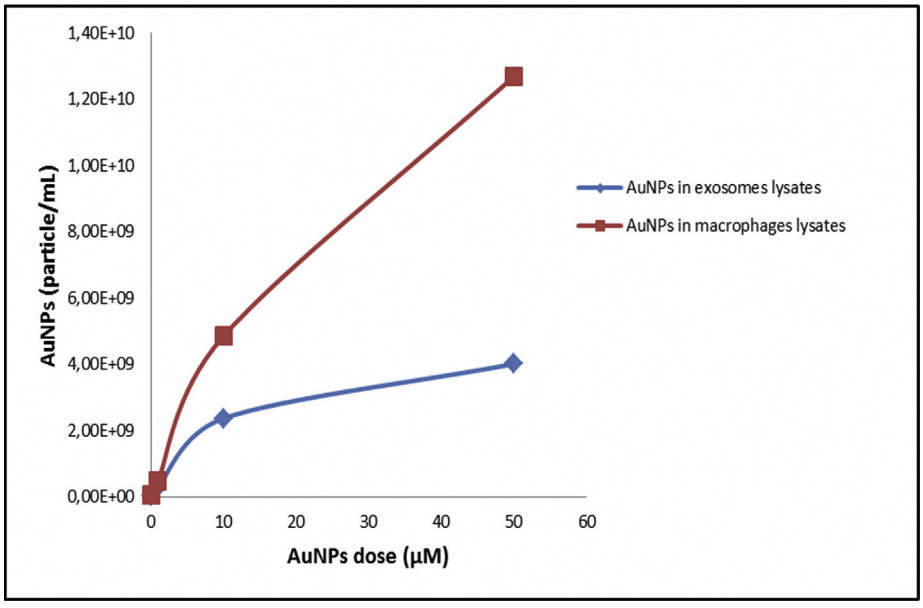

Fig. 6. AuNPs counts (particles/ml) in human macrophages and exosomes. (Red line) AuNPs counts (particles/ml) in lysates of human macrophages treated with AuNPs at 0, 0.1 1.0, 10 and 50 μM. (Blue line) AuNPs counts (particles/ml) in exosomes secreted by human macrophages treated with AuNPs at 0, 0.1 1.0, 10 and 50 μM. (For interpretation of the references to colour in this figure legend, the reader is referred to the web version of this article.)

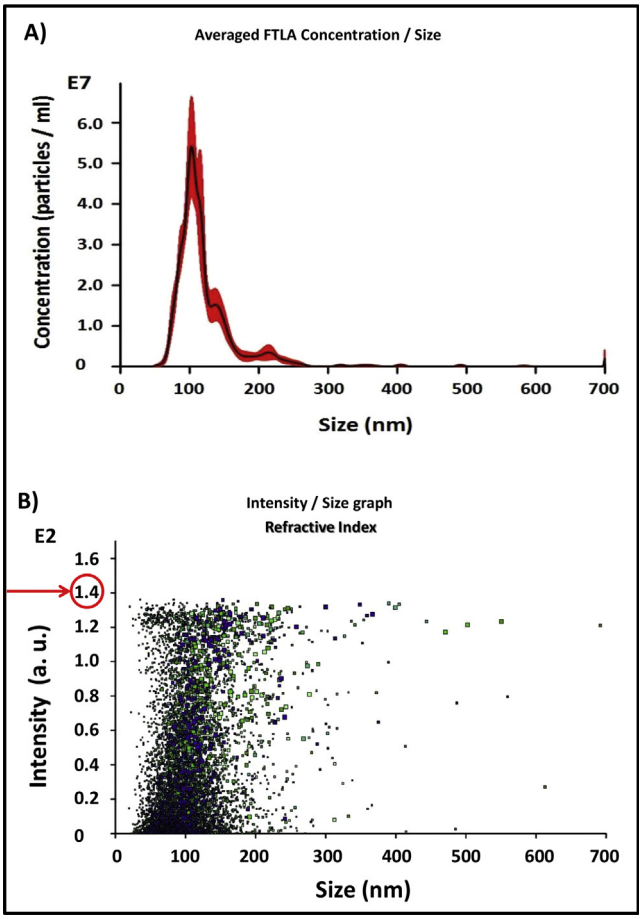

Fig. 8. Nanoparticle Tracking Analysis (NTA) of exosomes purified from primary human macrophages not treated with AuNPs (control). NTA for distribution, concentration (absolute count) and refractive index of exosomes released by human macrophages not treated with AuNPs.

mortality and the greatest exosomes secretion. To get to this result we previously performed time and dose response experiments with AuNPs (data not shown).

3.2. Laser scanning confocal microscopy (LSCM) analysis to verify AuNPs phagocytosis in human macrophages

The differentiated primary human macrophages were treated for 24 h with AuNPs at the concentration of 10 μM and analyzed through confocal microscopy, to verify the presence and distribution of AuNPs within macrophages.

The first analysis was to verify whether the AuNPs were able to emit fluorescence: when they are excited at wavelengths of 480–520 nm, the AuNPs emit fluorescence in the green (Fig. 2A).

We subsequently observed the presence of AuNPs within human macrophages treated by exciting the cells at the previously described wavelengths: Fig. 2C, 2C1, 2D clearly shows the presence of AuNPs in the cytoplasm of human macrophages compared to untreated macrophages in which there is no fluorescence emission (Fig. 2B, 2B1). Thus, LSCM analysis has shown that human macrophages are able to phagocytize AuNPs.

3.3. Transmission electron microscopy (TEM) analysis to verify the internalization of AuNPs by subcellular organelles of treated human macrophages

The use of electron microscopy allowed us to confirm the ability of human macrophages to phagocytize AuNPs. Following their differentiation, macrophages were treated for 24 h with AuNPs at the concentration of 10 μM.

The results show the presence of AuNPs in the cytoplasm of the treated macrophages. In particular, the images clearly reveal the proximity of AuNPs to the cell membrane (Fig. 3B) and their presence in the early endosomes (arrows in Fig. 3B) and/or in structures resembling the multivesicular body (MVB) (Fig. 3B1). The data show that the exosomes isolated from the treated cells are clearly associated to AuNPs, these observations allow to hypothesize that AuNPs were internalized by the cells, according to a typical absorption mechanism involving the clathrin-coated vesicles. These intraluminal vesicles (ILVs), which carry AuNPs, bud inward and pinch off into the lumen of the multivesicular bodies (MVBs). Ultimately, the MVBs move to the plasma membrane and exosomes carrying AuNPs out of the cells are secreted.

3.4. Characterization of exosomes isolated from human macrophages treated with AuNPs

The exosomes, secreted by human macrophages following 24 h treatment with 10 μM of AuNPs, were first characterized for the presence of typical exosomal markers (Tsg101, CD9 and CD81) by western blot analysis (Supplementary Fig. 1) and Nanoscale flow-cytometry (Cytoflex) (Supplementary Fig. 2). Western blot analysis showed that the exosomes isolated from the supernatants of AuNPs treated human macrophages equally expressed Tsg-101 (Supplementary Fig. 1). The exosomes were further characterized by Nanoscale flow-cytometry for CD81 and CD9, labeled respectively in APC (alloficocyanine) and PE (phycoerythrin) and the double positive events were counted and analyzed by the size (Supplementary Fig. 2). The results clearly confirmed the positivity for the typical exosome markers (CD9 and CD81).

3.5. Single Particle-Inductively Coupled Plasma-Mass Spectrometry (SP-ICP-MS) performances for the size and particle number concentration of AuNPs

In order to apply the SP-ICP-MS method for the direct characterization of AuNPs in macrophage and exosome lysates we obtained information on the number concentration of AuNPs and on diameter (D) in a very short time (60 s).

Supplementary Fig. 3 shows the diameter distribution of the standard of AuNPs at 20 nm in water (Supplementary Fig. 3A) and in RPMI + 10% of serum (Supplementary Fig. 3B), at the two time measurements at T0 and after 24 h (T24). Comparing the number concentration of the particles used and that measured with SP-ICP-MS, the recoveries were found to be 94% and 88% in water at T0 and T24 and 94% and 89% in RPMI + 10% of serum at T0 and T24, confirming good measurements accuracy. The measured D values were 20.5 ± 3.1 nm and 20.2 ± 3.2 nm in water at T0 and T24 and 19.5 ± 3.5 nm and 19.9 ± 3.3 nm in cell culture medium at T0 and T24; these values are in full agreement with the dimensions stated in the manufacturer's certificate. The LoD_{size} for AuNPs was approximately 10 nm in both water and cell culture medium. These results demonstrated the method was able to accurately detect, count and measure AuNPs, showing also that AuNPs did not dissolve and not aggregate in water and culture medium environments for 24 hrs.

3.6. Determination of AuNPs in human macrophages and exosomes by SP-ICP-MS

After demonstrating AuNPs stability over time in culture medium, the differentiated primary human macrophages were treated for 24 h with increasing concentrations of AuNPs (0.1, 1, 10 and 50 μM) and the macrophage-released exosomes were analyzed by SP-ICP-MS to detect the presence of AuNPs, after the standard ultracentrifugation rounds

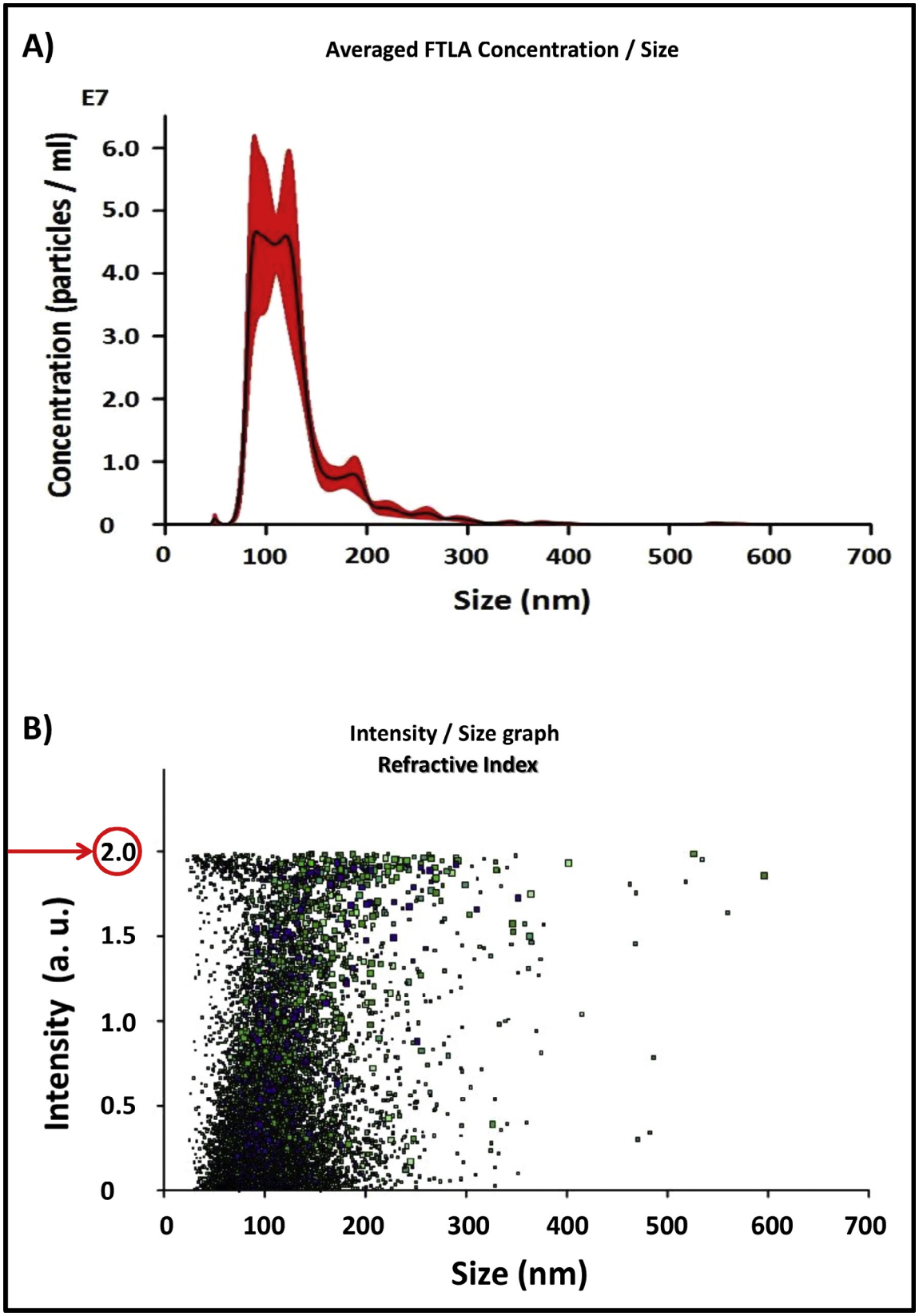

Fig. 9. Nanoparticle Tracking Analysis (NTA) of exosomes purified from primary human macrophages treated with AuNPs. NTA for distribution, concentration (absolute count) and refractive index of exosomes released by human macrophages treated with AuNPs.

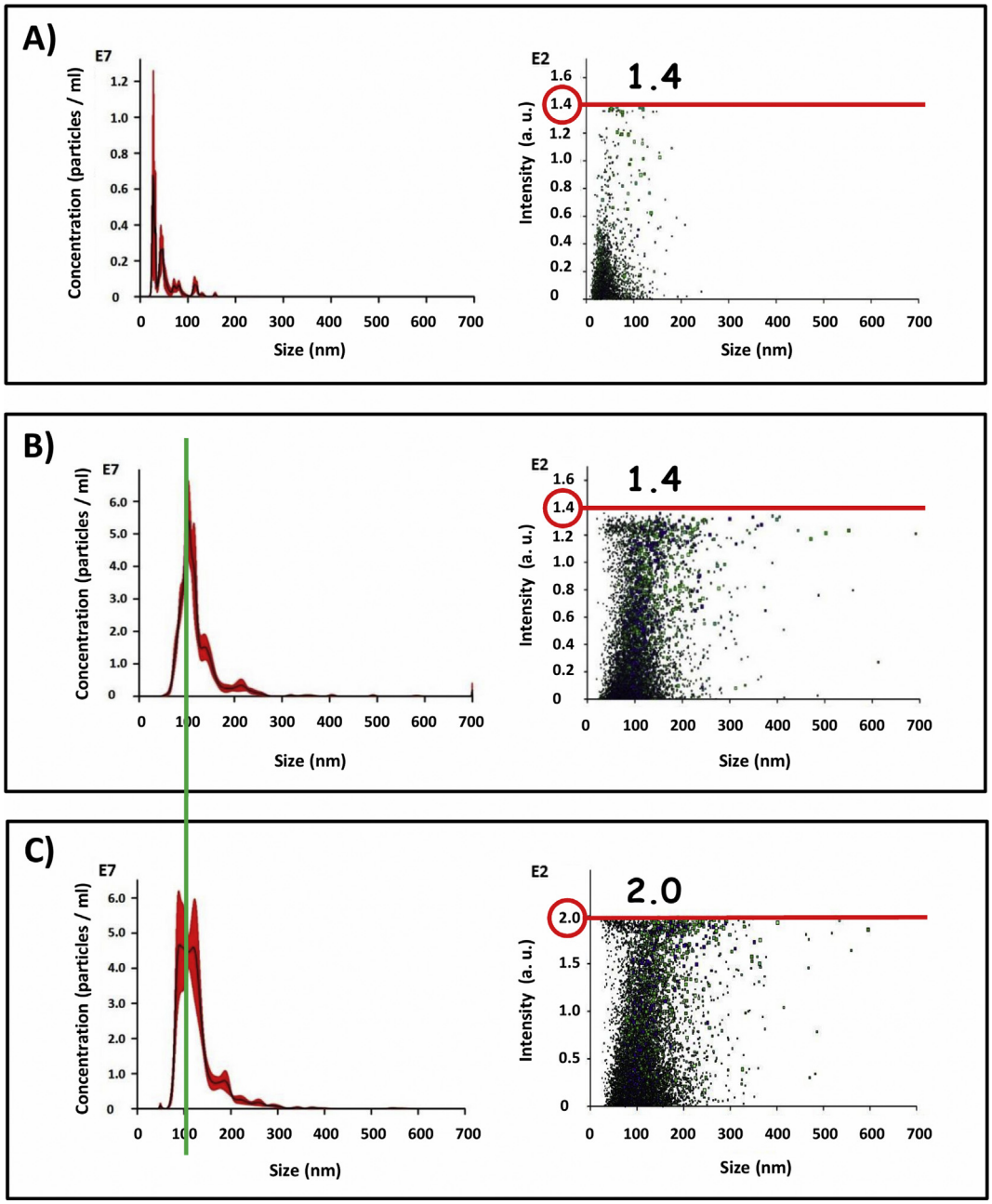

Fig. 10. Nanoparticle Tracking Analysis (NTA) for identifying AuNPs in exosomes. Summary representation of NTA for distribution, concentration (absolute count) and refractive index of: A) AuNPs diluted in water; B) exosomes released by human macrophages not treated with AuNPs (control); C) exosomes released by human macrophages treated with AuNPs.

[62].

Fig. 4 show the raw data obtained with SP-ICP-MS for AuNPs signals in control cells (0 μM; Fig. 4A) and in cells treated at doses of 0.1 μM, 1.0 μM, 10 μM and 50 μM (Fig. 4B–E). In Fig. 5, AuNPs signals are shown for control exosomes (0 μM; Fig. 5A) and for exosomes secreted by cells treated at doses of 0.1 μM, 1.0 μM, 10 μM and 50 μM (Fig. 5B–E). In the raw data of both Figs. 4 and 5, the frequency of spikes represented the number concentration of AuNPs (number of particles/ml), while the height of spikes (in cps) is proportional to the diameter (D value) of AuNPs.

The results expressed as particles/ml and D values (in nm) of AuNPs found in cell and exosome lysates are summarized in Table 2 and presented graphically in Fig. 6 as a function of dose increase.

There were no spikes in control samples of lysated cells (Fig. 4A) and exosomes (Fig. 5A) and this indicated that no AuNPs were present. The height of spikes, which was similar at different doses in the lysates of cells and exosomes (Fig. 4B–E and Fig. 5B–E), confirmed the presence of a narrow size distribution of particles with Au medium diameter of ca. 20 nm. Furthermore, the low BG in all the samples indicated the absence of dissolved Au ions. In particular, mean D values between 21.4 nm and 24.0 nm in cell lysates and between 20.5 nm and 22.0 nm in exosomes lysates at all doses were found (Table 2).

Moreover, a higher number of AuNPs spikes in cell and exosome lysates was observed when the treatment doses increased (Fig. 4B–E and Fig. 5B–E). In particular, in macrophage lysates the number of AuNPs increased of ca. 10-times between 0.1 and 1 μM and 1–10 μM doses, as compared with only 3-times between 10 and 50 μM (Table 2). Also in lysed exosomes the number of AuNPs increased proportionally between 0.1 and 1.0–10 μM doses, whilst the increment was only 1.7-times between 10 and 50 μM (Table 2). The curves of Fig. 6 clearly

show a saturation phase at the highest dose, more pronounced for exosomes than for macrophages.

We also calculated the fraction of AuNPs in exosomes lysates (F_{exo} %) using the following equation: $F_{exo}\ \% = (N_{out}/N_{in}) \times 100$ where N_{out} is the number of AuNPs secreted in the exosomes and N_{in} is the number of AuNPs present in the macrophages.

The values of F_{exo} % were: 42% at 0.1 μM, 56% at 1.0 μM, 49% at 10 μM, and 32% at 50 μM. These data suggested that the fraction of AuNPs eliminated from the cells through the exosomes was of ca. 50% at all doses, and it was lower at the highest dose. However, we were not in the condition to investigate further times in order to provide data on the whole elimination of AuNPs from macrophages through exosomes, inasmuch as continuative 5 days culture of primary macrophages is a limit condition; after that the culture medium has to be changed and/or cells detached and seeded again.

3.7. Primary human macrophages release AuNPs through exosomes: NTA (Nanoparticle Tracking Analysis)

The exosomes were isolated by serial ultracentrifugation following treatment of primary human macrophages with AuNPs (Fig. 1). The exosomes were analyzed by NTA (Nanosight) for distribution, concentration (absolute count) and refractive index. With this technique the nanovesicles from 10 nm up to 1000 nm are visualized in real time through the Brownian movement. We evaluated the real 20 nm size of AuNPs diluted in water, as can be seen in the graphs in Fig. 7. The AuNPs have not a homogeneous distribution, but the peak of the elementary population is visible and predominant with a size of 20 nm and a maximum refractive index of 1,4 a.u. (arbitrary unit). The presence of the dimers can be explained by a phenomenon of aggregation of the gold nanoparticles dependent on dilution. Despite the presence of these presumed aggregates, NanoSight analysis provided a high resolution number weighted size distribution to accurately measure the size and concentration of the primary particle population [64]. NTA is reliable in sizes below 50 nm in particular with gold and silver samples due to their high refractive index, indeed it has the sensitivity to measure high scattering materials like gold and silver down to 10 nm [64].

The exosomes isolated from the primary human macrophages not treated with the AuNPs (Fig. 8A and B) have an average size of 122.4 ± 1.6 nm (Fig. 8A) and a maximum refractive index equal to 1.4 a.u. (Fig. 8B).

The exosomes isolated from human macrophages treated with AuNPs (Fig. 9A and B) have average dimensions of 127.0 ± 3.8 nm (Fig. 9A) and a refractive index up to a maximum of 2.0 a.u. (Fig. 9B), therefore higher by a value of 0.6 than the controls. With these results we show for the first time that NTA can be used for the identification of the exosomes containing a nanomaterial such as AuNPs: in fact, the exosomes containing AuNPs have an increase in size and present a shift of the dimensional peak with consequent increase in the index of refraction as compared to the exosomes released by untreated macrophages (Fig. 10), strongly supporting the presence of AuNPs in the exosomes released by macrophages. In conclusion, the refractive index provides a useful and easy method to show the presence of nanomaterials, such as AuNPs, within the exosomes; this achievement was obtained thanks to the light diffusion intensity correlated to the sample.

4. Discussion

This study shows the ability of primary peripheral blood monocytes derived-human macrophages, to endocytose gold nanoparticles (AuNPs) and release them into the extracellular environment through exosomes. We decided to use 20 nm AuNPs because of its physical and optical properties that allowed multi-parametric analysis through qualitative and quantitative techniques, such as TEM (Transmission Electron Microscope), LSCM (Laser scanning confocal microscopy), NTA (Nanoparticle Tracking Analysis) and SP-ICP-MS (Single Particles-Inductively Coupled Plasma-Mass Spectrometry); thus offering specific advantages and different level of information. We propose to combine these techniques using a multi-instrumental approach [65] in order to set up more suitable approach aimed at measuring the level of nanoparticle (NPs) uptake by scavenger cells, such as macrophages, and the levels of nanoparticles elimination by exosomes. However, we used AuNPs for the high interest in their clinical use as well, and therefore as a prototype of nanoparticles destined to a clinical use.

The LSCM and TEM analyses clearly demonstrated that human macrophages are able to endocytose nanoparticles such as AuNPs. Moreover, morphological examination showed that the AuNPs were concentrated on the inner membrane of a structure similar to the early endosomes or MVBs, from which the exosomes originate. In fact, we hypothesized that the AuNPs, following their internalization by macrophages, are directed towards the endosomal pathway. The AuNPs are packaged into the intraluminal vesicles (ILVs) and then into the lumen of multivesicular bodies (MVBs) which, merging with the plasma membrane, release the exosomes taking the AuNPs to the extracellular microenvironment.

The use of SP-IC-MS confirmed this observation and identified for the first time AuNPs also in lysed exosomes, in a dose-dependent manner.

To validate the method with the technique of the SP-ICP-MS we demonstrated that it was possible to accurately calculate (recoveries from 88 to 94%) the AuNPs and to measure directly into the lysates their D (diameter) values with high sensitivity levels (LoD_{size} of 10 nm). Moreover, we show here that the 20 nm size remained unchanged after the cellular uptake of AuNPs and the release within exosomes; and with an irrelevant background in all samples suggesting the absence of dissolved Au ions.

The results of SP-ICP-MS showed that the 20 nm AuNPs were phagocytized by primary human macrophages in a dose-dependent manner and were secreted by the cells through the exosomes in relation to the dose. In both cells and exosomes, this relationship has reached a limit at the maximum dose.

The percentage of AuNPs released extracellularly with the exosomes ranged between 32% and 59% of the AuNPs uptaken by macrophages, supporting a real role of exosomes in eliminating extracellularly the majority of the scavenged AuNPs.

A very important add of this study is the demonstration that NTA can be used to verify the presence of NPs within intact exosomes. This result was obtained by the ensemble of two data: (i) the increase in the exosomes diameter and (ii) the difference in the refractive index between exosomes released by AuNPs-treated macrophages and those from untreated cells. The use of complementary techniques, such as SP-ICP-MS and NTA, highlighted two different information: (i) the SP-ICP-MS clearly demonstrated the composition and concentration of nanomaterial detectable in the lysed exosomes, i.e. the number and the size of NPs, distinguishing them from the dissolved form of the nanomaterial, while (ii) the NanoSight allows the measurement of the distribution, concentration and index of refraction of the NPs containing intact exosomes once suspended in a liquid, through the Brownian movements and the refractive index.

The nanomaterials that enter the body through air, water, food, clothes are delivered to the various organs through the bloodstream, can accumulate in organs or tissues and be partially or completely eliminated through urine and feces [2]. Blood (platelets, monocytes, endothelial cells), urine and feces therefore represent indicators of exposure [22]. Our results suggest for the first time that nanomaterials getting to tissues are scavenged by macrophages that then release them extracellularly through exosomes. The fate of nanomaterial-containing exosomes may well be that they may transfer the nanomaterial to other cells in a paracrine way; but also that the exosomes with the nanomaterial may be spilled over the body through the bloodstream. Which in turn means that the analysis of circulating exosomes isolated from subjects exposed to nanomaterials may represent an entirely new

indicator in toxicology. In fact our previous work has shown that exosomes may be purified and analyzed in the plasma of both healthy individuals and patients [63,66]. Therefore, exosomes may represent biomarkers of exposure to nanomaterials, such as e.g. AuNPs, Titanium Dioxide, Silver, Iron, etc.

Given that the exosomes present in body fluids (blood, saliva, cerebrospinal fluid, maternal milk and urine) are able to shuttle various molecules, including chemicals [46,47,63,67], their isolation from the peripheral blood and the analysis by NTA and SP-ICP-MS analysis can represent a useful tool for the early identification of nanomaterials in exposed subjects, otherwise not detectable with the currently used diagnostic technologies. The NTA technique is easy to use and allows to evaluate the presence of nanomaterials within the exosomes in a short time, with accuracy and precision, representing a simple, economic and non-invasive diagnostic tool. Considering that the NTA technique does not allow to identify the type of nanomaterial present, the use of the SP-ICP-MS technique is used to characterize the metallic nanomaterials present in the exosomes.

This work therefore addresses the too many unmet questions in the *in vivo* evaluation of toxicity, exposure and risk to nanomaterials [68,69]: to date we are not fully aware of the physico-chemical, the intrinsic and acquired properties of nanomaterials, nor of the impact of nanomaterials on health and the environment [68,70]. Furthermore, there are no standard methodologies or exposure biomarkers that allow the definition of assessment parameters for health exposure dose [68], so it is not possible to clearly define a health surveillance protocol.

Therefore, our observations represent a valid system for determining the *in vivo* nanotoxicity correlated to nanomaterials in order to provide health surveillance for workers exposed to nanomaterials: the identification of nanomaterials in exosomes isolated from the blood of exposed subjects can allow identification of doses potentially dangerous for human health and provide more information on the pharmacokinetics and pharmacodynamics of the nanomaterials themselves.

Of course nanoparticles-containing exosomes may be delivered to virtually all the body compartments. However, it is mandatory that there are organs that when targeted by the nanoparticles-containing exosomes have less chance to quickly free from them. Between the many the brain risks to be organ with the fewest options to eliminate the nanoparticles-containing exosomes. In fact, on one hand we know from the clinical oncology that brain tumors do not metastasize outside the brain, while virtually all the other tumors metastasize to the brain. However, recent evidence further support it inasmuch as it is hard to detect molecules in the blood of patients with primary brain tumors, while tumor associated molecules may be found in the cerebrospinal fluid [71]. This makes conceivable that from the blood any kind of molecule may enter the brain but it is highly hard that it may get out from it. Based on this consideration, our study further suggests that exosomes, given their ability to transport nanomaterials, shown in our study, and to cross the brain barrier [72], could be able to release into the central nervous system the nanomaterials of people exposed to them, with a progressive accumulation of the nanomaterial in a system that is not able to eliminate it, thus leading to neurotoxicity and over time to neurodegeneration.

In conclusion, the results and the methodologies used in this study first provide the evidence that our body scavenge the nanomaterial and eliminate them through exosomes. Then, we provide a new technical approach helpful in assessing the circulation of the nanomaterials through the body, and to monitor the exposure to nanomaterials for risk assessment, necessary for planning exposure controls.

Competing interests

The authors declare that they have no competing interests.

Funding

This work was supported by Regione Lazio FILAS [grant number RU 2014-2041 FascJ9L].

Appendix A. Supplementary material

Supplementary data to this article can be found online at https://doi.org/10.1016/j.ejpb.2019.02.014.

References

[1] Nanomaterials – ECHA, n.d. https://echa.europa.eu/regulations/nanomaterials (accessed July 24, 2018).
[2] G. Oberdörster, E. Oberdörster, J. Oberdörster, Nanotoxicology: an emerging discipline evolving from studies of ultrafine particles, Environ. Health Perspect. 113 (2005) 823–839.
[3] C. Gerber, H.P. Lang, How the doors to the nanoworld were opened, Nat. Nanotechnol. 1 (2006) 3–5, https://doi.org/10.1038/nnano.2006.70.
[4] M.A. Dobrovolskaia, S.E. McNeil, Immunological properties of engineered nanomaterials, Nat. Nanotechnol. 2 (2007) 469–478, https://doi.org/10.1038/nnano.2007.223.
[5] M.A. Dobrovolskaia, D.R. Germolec, J.L. Weaver, Evaluation of nanoparticle immunotoxicity, Nat. Nanotechnol. 4 (2009) 411–414, https://doi.org/10.1038/nnano.2009.175.
[6] D.B. Warheit, Debunking some misconceptions about nanotoxicology, Nano Lett. 10 (2010) 4777–4782, https://doi.org/10.1021/nl103432w.
[7] Commission Recommendation of 18 October 2011 on the definition of nanomaterial Text with EEA relevance, 2011. http://data.europa.eu/eli/reco/2011/696/oj/eng (accessed July 26, 2018).
[8] Risk assessment of Products of Nanotechnologies, n.d. http://ec.europa.eu/health/ph_risk/committees/04_scenihr/docs/scenihr_o_023.pdf.
[9] A.A. Shvedova, V.E. Kagan, B. Fadeel, Close encounters of the small kind: adverse effects of man-made materials interfacing with the nano-cosmos of biological systems, Annu. Rev. Pharmacol. Toxicol. 50 (2010) 63–88, https://doi.org/10.1146/annurev.pharmtox.010909.105819.
[10] B. Wang, X. He, Z. Zhang, Y. Zhao, W. Feng, Metabolism of nanomaterials *in vivo*: blood circulation and organ clearance, Acc. Chem. Res. 46 (2013) 761–769, https://doi.org/10.1021/ar2003336.
[11] E. Sadauskas, G. Danscher, M. Stoltenberg, U. Vogel, A. Larsen, H. Wallin, Protracted elimination of gold nanoparticles from mouse liver, Nanomed. Nanotechnol. Biol. Med. 5 (2009) 162–169, https://doi.org/10.1016/j.nano.2008.11.002.
[12] M. Longmire, P.L. Choyke, H. Kobayashi, Clearance properties of nano-sized particles and molecules as imaging agents: considerations and caveats, Nanomed 3 (2008) 703–717, https://doi.org/10.2217/17435889.3.5.703.
[13] R.A. Petros, J.M. DeSimone, Strategies in the design of nanoparticles for therapeutic applications, Nat. Rev. Drug Discov. 9 (2010) 615–627, https://doi.org/10.1038/nrd2591.
[14] H. Koo, M.S. Huh, I.-C. Sun, S.H. Yuk, K. Choi, K. Kim, et al., In Vivo targeted delivery of nanoparticles for theranosis, Acc. Chem. Res. 44 (2011) 1018–1028, https://doi.org/10.1021/ar2000138.
[15] Y. Pan, A. Leifert, D. Ruau, S. Neuss, J. Bornemann, G. Schmid, et al., Gold nanoparticles of diameter 1.4 nm trigger necrosis by oxidative stress and mitochondrial damage, Small 5 (2009) 2067–2076, https://doi.org/10.1002/smll.200900466.
[16] S. Sharifi, S. Behzadi, S. Laurent, M. Laird Forrest, P. Stroeve, M. Mahmoudi, Toxicity of nanomaterials, Chem. Soc. Rev. 41 (2012) 2323–2343, https://doi.org/10.1039/C1CS15188F.
[17] V. Sharma, P. Singh, A.K. Pandey, A. Dhawan, Induction of oxidative stress, DNA damage and apoptosis in mouse liver after sub-acute oral exposure to zinc oxide nanoparticles, Mutat. Res. Toxicol. Environ. Mutagen. 745 (2012) 84–91, https://doi.org/10.1016/j.mrgentox.2011.12.009.
[18] A. Manke, L. Wang, Y. Rojanasakul, Mechanisms of nanoparticle-induced oxidative stress and toxicity, BioMed. Res. Int. 2013 (2013) 1–15, https://doi.org/10.1155/2013/942916.
[19] E. Huerta-García, J.A. Pérez-Arizti, S.G. Márquez-Ramírez, N.L. Delgado-Buenrostro, Y.I. Chirino, G.G. Iglesias, et al., Titanium dioxide nanoparticles induce strong oxidative stress and mitochondrial damage in glial cells, Free Radic. Biol. Med. 73 (2014) 84–94, https://doi.org/10.1016/j.freeradbiomed.2014.04.026.
[20] I. Inkielewicz-Stepniak, K. Niska, K. Pyszka, C. Tukaj, M. Wozniak, M. Radomski, Titanium dioxide nanoparticles enhance production of superoxide anion and alter the antioxidant system in human osteoblast cells, Int. J. Nanomed. 1095 (2015), https://doi.org/10.2147/IJN.S73557.
[21] M.-J. Favé, F.C. Lamaze, D. Soave, A. Hodgkinson, H. Gauvin, V. Bruat, et al., Gene-by-environment interactions in urban populations modulate risk phenotypes, Nat. Commun. 9 (2018), https://doi.org/10.1038/s41467-018-03202-2.
[22] G. Oberdörster, A. Maynard, K. Donaldson, V. Castranova, J. Fitzpatrick, K. Ausman, et al., Principles for characterizing the potential human health effects from exposure to nanomaterials: elements of a screening strategy, Part Fibre Toxicol. 2 (2005) 8, https://doi.org/10.1186/1743-8977-2-8.
[23] K. Donaldson, R. Aitken, L. Tran, V. Stone, R. Duffin, G. Forrest, et al., Carbon nanotubes: a review of their properties in relation to pulmonary toxicology and

workplace safety, Toxicol. Sci. Off. J. Soc. Toxicol. 92 (2006) 5–22, https://doi.org/10.1093/toxsci/kfj130.
[24] A. Seabra, N. Durán, Nanotoxicology of metal oxide nanoparticles, Metals 5 (2015) 934–975, https://doi.org/10.3390/met5020934.
[25] M.A.K. Abdelhalim, B.M. Jarrar, Gold nanoparticles induced cloudy swelling to hydropic degeneration, cytoplasmic hyaline vacuolation, polymorphism, binucleation, karyopyknosis, karyolysis, karyorrhexis and necrosis in the liver, Lipids Health Dis. 10 (2011) 166, https://doi.org/10.1186/1476-511X-10-166.
[26] Y. Song, X. Li, X. Du, Exposure to nanoparticles is related to pleural effusion, pulmonary fibrosis and granuloma, Eur. Respir. J. 34 (2009) 559–567, https://doi.org/10.1183/09031936.00178308.
[27] J.I. Phillips, F.Y. Green, J.C.A. Davies, J. Murray, Pulmonary and systemic toxicity following exposure to nickel nanoparticles, Am. J. Ind. Med. n/a-n/a (2010), https://doi.org/10.1002/ajim.20855.
[28] P. Møller, D.V. Christophersen, D.M. Jensen, A. Kermanizadeh, M. Roursgaard, N.R. Jacobsen, et al., Role of oxidative stress in carbon nanotube-generated health effects, Arch. Toxicol. 88 (2014) 1939–1964, https://doi.org/10.1007/s00204-014-1356-x.
[29] Y. Chen, G. Li, Y. Liu, V.P. Werth, K.J. Williams, M.-L. Liu, Translocation of endogenous danger signal hmgb1 from nucleus to membrane microvesicles in macrophages: translocation of nuclear HMGB1 to membrane microvesicles, J. Cell Physiol. 231 (2016) 2319–2326, https://doi.org/10.1002/jcp.25352.
[30] C. Cordazzo, S. Petrini, T. Neri, S. Lombardi, Y. Carmazzi, R. Pedrinelli, et al., Rapid shedding of proinflammatory microparticles by human mononuclear cells exposed to cigarette smoke is dependent on Ca2+ mobilization, Inflamm. Res. 63 (2014) 539–547, https://doi.org/10.1007/s00011-014-0723-7.
[31] M. Li, D. Yu, K.J. Williams, M.-L. Liu, Tobacco smoke induces the generation of procoagulant microvesicles from human monocytes/macrophages, Arterioscler. Thromb. Vasc. Biol. 30 (2010) 1818–1824, https://doi.org/10.1161/ATVBAHA.110.209577.
[32] T. Neri, L. Pergoli, S. Petrini, L. Gravendonk, C. Balia, V. Scalise, et al., Particulate matter induces prothrombotic microparticle shedding by human mononuclear and endothelial cells, Toxicol. In Vitro 32 (2016) 333–338, https://doi.org/10.1016/j.tiv.2016.02.001.
[33] F. Sabatier, L. Camoin-Jau, F. Anfosso, J. Sampol, F. Dignat-George, Circulating endothelial cells, microparticles and progenitors: key players towards the definition of vascular competence, J. Cell Mol. Med. 13 (2009) 454–471, https://doi.org/10.1111/j.1582-4934.2008.00639.x.
[34] D. Burger, R.M. Touyz, Cellular biomarkers of endothelial health: microparticles, endothelial progenitor cells, and circulating endothelial cells, J Am. Soc. Hypertens. 6 (2012) 85–99, https://doi.org/10.1016/j.jash.2011.11.003.
[35] C.-J. Li, Y. Liu, Y. Chen, D. Yu, K.J. Williams, M.-L. Liu, Novel Proteolytic microvesicles released from human macrophages after exposure to tobacco smoke, Am. J. Pathol. 182 (2013) 1552–1562, https://doi.org/10.1016/j.ajpath.2013.01.035.
[36] M. Folkesson, C. Li, S. Frebelius, J. Swedenborg, D. Wågsäter, K.J. Williams, et al., Proteolytically active ADAM10 and ADAM17 carried on membrane microvesicles in human abdominal aortic aneurysms, Thromb. Haemost. 114 (2015) 1165–1174, https://doi.org/10.1160/TH14-10-0899.
[37] H. Liu, L. Ding, Y. Zhang, S. Ni, Circulating endothelial microparticles involved in lung function decline in a rat exposed in cigarette smoke maybe from apoptotic pulmonary capillary endothelial cells, J. Thorac. Dis. 6 (2014) 649–655, https://doi.org/10.3978/j.issn.2072-1439.2014.06.26.
[38] B.J. Benedikter, E.F.M. Wouters, P.H.M. Savelkoul, G.G.U. Rohde, F.R.M. Stassen, Extracellular vesicles released in response to respiratory exposures: implications for chronic disease, J. Toxicol. Environ. Health B Crit. Rev. (2018) 1–19, https://doi.org/10.1080/10937404.2018.1466380.
[39] G. Andreola, L. Rivoltini, C. Castelli, V. Huber, P. Perego, P. Deho, et al., Induction of lymphocyte apoptosis by tumor cell secretion of FasL-bearing microvesicles, J. Exp. Med. 195 (2002) 1303–1316.
[40] G. Camussi, M.-C. Deregibus, S. Bruno, C. Grange, V. Fonsato, C. Tetta, Exosome/microvesicle-mediated epigenetic reprogramming of cells, Am. J. Cancer Res. 1 (2011) 98–110.
[41] E.N.M. Nolte-t Hoen, H.P.J. Buermans, M. Waasdorp, W. Stoorvogel, M.H.M. Wauben, P.A.C. Hoen, Deep sequencing of RNA from immune cell-derived vesicles uncovers the selective incorporation of small non-coding RNA biotypes with potential regulatory functions, Nucleic Acids Res. 40 (2012) 9272–9285, https://doi.org/10.1093/nar/gks658.
[42] A. Canitano, G. Venturi, M. Borghi, M.G. Ammendolia, S. Fais, Exosomes released in vitro from Epstein-Barr virus (EBV)-infected cells contain EBV-encoded latent phase mRNAs, Cancer Lett. 337 (2013) 193–199, https://doi.org/10.1016/j.canlet.2013.05.012.
[43] F. Properzi, M. Logozzi, H. Abdel-Haq, C. Federici, L. Lugini, T. Azzarito, et al., Detection of exosomal prions in blood by immunochemistry techniques, J. Gen. Virol. 96 (2015) 1969–1974, https://doi.org/10.1099/vir.0.000117.
[44] C. Théry, K.W. Witwer, E. Aikawa, M.J. Alcaraz, J.D. Anderson, R. Andriantsitohaina, et al., Minimal information for studies of extracellular vesicles 2018 (MISEV2018): a position statement of the International Society for Extracellular Vesicles and update of the MISEV2014 guidelines, J. Extracell. Vesicles 7 (2018) 1535750, https://doi.org/10.1080/20013078.2018.1535750.
[45] S. Fais, L. O'Driscoll, F.E. Borras, E. Buzas, G. Camussi, F. Cappello, et al., Evidence-based clinical use of nanoscale extracellular vesicles in nanomedicine, ACS Nano 10 (2016) 3886–3899, https://doi.org/10.1021/acsnano.5b08015.
[46] C. Federici, F. Petrucci, S. Caimi, A. Cesolini, M. Logozzi, M. Borghi, et al., Exosome release and low ph belong to a framework of resistance of human melanoma cells to cisplatin, PLoS ONE 9 (2014) e88193, https://doi.org/10.1371/journal.pone.0088193.
[47] E. Iessi, M. Logozzi, L. Lugini, T. Azzarito, C. Federici, E.P. Spugnini, et al., Acridine Orange/exosomes increase the delivery and the effectiveness of Acridine Orange in human melanoma cells: a new prototype for theranostics of tumors, J. Enzyme Inhib. Med. Chem. 32 (2017) 648–657, https://doi.org/10.1080/14756366.2017.1292263.
[48] H. Zhao, A. Achreja, E. Iessi, M. Logozzi, D. Mizzoni, R. Di Raimo, et al., The key role of extracellular vesicles in the metastatic process, Biochim. Biophys. Acta BBA – Rev. Cancer 1869 (2018) 64–77, https://doi.org/10.1016/j.bbcan.2017.11.005.
[49] S.J. Gould, G. Raposo, As we wait: coping with an imperfect nomenclature for extracellular vesicles, J. Extracell. Vesicles 2 (2013) 20389, https://doi.org/10.3402/jev.v2i0.20389.
[50] M. Garofalo, H. Saari, P. Somersalo, D. Crescenti, L. Kuryk, L. Aksela, et al., Antitumor effect of oncolytic virus and paclitaxel encapsulated in extracellular vesicles for lung cancer treatment, J. Control Release Off. J. Control Release Soc. 283 (2018) 223–234, https://doi.org/10.1016/j.jconrel.2018.05.015.
[51] A. Goes, G. Fuhrmann, Biogenic and biomimetic carriers as versatile transporters to treat infections, ACS Infect. Dis. 4 (2018) 881–892, https://doi.org/10.1021/acsinfecdis.8b00030.
[52] M. Zhu, Y. Li, J. Shi, W. Feng, G. Nie, Y. Zhao, Exosomes as extrapulmonary signaling conveyors for nanoparticle-induced systemic immune activation, Small 8 (2012) 404–412, https://doi.org/10.1002/smll.201101708.
[53] S. Fais, M. Overholtzer, Cell-in-cell phenomena in cancer, Nat. Rev. Cancer 18 (2018) 758–766, https://doi.org/10.1038/s41568-018-0073-9.
[54] S. Fais, F. Luciani, M. Logozzi, S. Parlato, F. Lozupone, Linkage between cell membrane proteins and actin-based cytoskeleton: the cytoskeletal-driven cellular functions, Histol. Histopathol. 15 (2000) 539–549, https://doi.org/10.14670/HH-15.539.
[55] S. Fais, V.L. Burgio, M.R. Capobianchi, S. Gessani, F. Pallone, F. Belardelli, The biological relevance of polykaryons in the immune response, Immunol. Today 18 (1997) 522–527.
[56] S. Fais, F. Pallone, Inability of normal human intestinal macrophages to form multinucleated giant cells in response to cytokines, Gut 37 (1995) 798–801.
[57] V.L. Burgio, S. Fais, M. Boirivant, A. Perrone, F. Pallone, Peripheral monocyte and naive T-cell recruitment and activation in Crohn's disease, Gastroenterology 109 (1995) 1029–1038.
[58] A. Liu, B. Ye, Application of gold nanoparticles in biomedical researches and diagnosis, Clin. Lab. 59 (2013) 23–36.
[59] H.E. Pace, N.J. Rogers, C. Jarolimek, V.A. Coleman, C.P. Higgins, J.F. Ranville, Determining transport efficiency for the purpose of counting and sizing nanoparticles via single particle inductively coupled plasma mass spectrometry, Anal. Chem. 83 (2011) 9361–9369, https://doi.org/10.1021/ac201952t.
[60] V. Felice, F. Cappello, A. Montalbano, N.M. Ardizzone, A. Luca, F. Macaluso, et al., HSP90 and eNOS partially co-localize and change cellular localization in relation to different ECM components in 2D and 3D cultures of adult rat cardiomyocytes, Biol. Cell 99 (2007) 689–699, https://doi.org/10.1042/BC20070043.
[61] F. Bucchieri, A. Pitruzzella, A. Fucarino, A.M. Gammazza, C.C. Bavisotto, V. Marcianò, et al., Functional characterization of a novel 3D model of the epithelial-mesenchymal trophic unit, Exp. Lung Res. 43 (2017) 82–92, https://doi.org/10.1080/01902148.2017.1303098.
[62] C. Théry, L. Zitvogel, S. Amigorena, Exosomes: composition, biogenesis and function, Nat. Rev. Immunol. 2 (2002) 569–579, https://doi.org/10.1038/nri855.
[63] M. Logozzi, D.F. Angelini, E. Iessi, D. Mizzoni, R. Di Raimo, C. Federici, et al., Increased PSA expression on prostate cancer exosomes in in vitro condition and in cancer patients, Cancer Lett. 403 (2017) 318–329, https://doi.org/10.1016/j.canlet.2017.06.036.
[64] Malvern Instruments Limited, Gold Nanoparticle Applications and Characterization by Nanoparticle Tracking Analysis, (2016).
[65] C.L. Geraci, V. Castranova, Challenges in assessing nanomaterial toxicology: a personal perspective: Challenges in assessing nanomaterial toxicology, Wiley Interdiscip. Rev. Nanomed. Nanobiotechnol. 2 (2010) 569–577, https://doi.org/10.1002/wnan.108.
[66] M. Logozzi, A. De Milito, L. Lugini, M. Borghi, L. Calabrò, M. Spada, et al., High levels of exosomes expressing CD63 and caveolin-1 in plasma of melanoma patients, PLoS One 4 (2009) e5219, https://doi.org/10.1371/journal.pone.0005219.
[67] S. Fais, M. Logozzi, L. Lugini, C. Federici, T. Azzarito, N. Zarovni, et al., Exosomes: the ideal nanovectors for biodelivery, Biol. Chem. 394 (2013) 1–15, https://doi.org/10.1515/hsz-2012-0236.
[68] J.S. Tsuji, A.D. Maynard, P.C. Howard, J.T. James, C.-W. Lam, D.B. Warheit, et al., Research strategies for safety evaluation of nanomaterials, part IV: risk assessment of nanoparticles, Toxicol. Sci. Off. J. Soc. Toxicol. 89 (2006) 42–50, https://doi.org/10.1093/toxsci/kfi339.
[69] P.A. Schulte, C.L. Geraci, V. Murashov, E.D. Kuempel, R.D. Zumwalde, V. Castranova, et al., Occupational safety and health criteria for responsible development of nanotechnology, J. Nanoparticle Res. Interdiscip. Forum Nanoscale Sci. Technol. 16 (2014) 2153, https://doi.org/10.1007/s11051-013-2153-9.
[70] I. Iavicoli, V. Leso, M. Manno, P.A. Schulte, Biomarkers of nanomaterial exposure and effect: current status, J. Nanoparticle Res. 16 (2014), https://doi.org/10.1007/s11051-014-2302-9.
[71] A.M. Miller, R.H. Shah, E.I. Pentsova, M. Pourmaleki, S. Briggs, N. Distefano, et al., Tracking tumour evolution in glioma through liquid biopsies of cerebrospinal fluid, Nature 565 (2019) 654–658, https://doi.org/10.1038/s41586-019-0882-3.
[72] M. Shi, L. Sheng, T. Stewart, C.P. Zabetian, J. Zhang, New windows into the brain: Central nervous system-derived extracellular vesicles in blood, Prog. Neurobiol. (2019), https://doi.org/10.1016/j.pneurobio.2019.01.005.